Studies on the Structure of the G-Protein-Coupled Receptor Rhodopsin Including the Putative G-Protein Binding Site in Unactivated and Activated Forms†

Philip L. Yeagle,* Gregory Choi, and Arlene D. Albert

Department of Molecular and Cell Biology, University of Connecticut, Storrs, Connecticut 06269

Received May 9, 2001; Revised Manuscript Received June 25, 2001

ABSTRACT: Activation of G-protein coupled receptors (GPCR) is not yet understood. A recent structure showed most of rhodopsin in the ground (not activated) state of the GPCR, but the cytoplasmic face, which couples to the G protein in signal transduction, was not well-defined. We have determined an experimental three-dimensional structure for rhodopsin in the unactivated state, which shows good agreement with the crystal structure in the transmembrane domain. This new structure defines the cytoplasmic face of rhodopsin. The G-protein binding site can be mapped. The same experimental approach yields a preliminary structure of the cytoplasmic face in the activated (metarhodopsin II) receptor. Differences between the two structures suggest how the receptor is activated to couple with transducin.

Rhodopsin belongs to the large family of G-protein coupled receptors controlling a wide variety of signal transduction. Circular dichroism studies (*1*), primary sequence (*2*), and a low-resolution structure from two-dimensional crystals (*3*, *4*) show that the transmembrane domain of bovine rhodopsin is a seven-helix bundle. X-ray crystallography elegantly defined the seven-helix bundle and intradiskal face of rhodopsin (not activated) at high-resolution (*5*).

Upon light activation, the G protein, transducin, binds to the cytoplasmic face of rhodopsin and initiates visual signal transduction. Structures of the cytoplasmic face for both rhodopsin (not activated) and metarhodopsin II (meta II, the activated form of the receptor) are required to understand this process. The crystal structure provides limited information on the cytoplasmic face of rhodopsin. Many residues from that region are missing from the structure and *B*-factors are high for other residues in the cytoplasmic face. Meta II[1] poses additional difficulties. The crystals of rhodopsin decompose upon exposure to light (*6*) and cannot be used to determine the meta II structure. Meta II is transient and consequently not readily crystallized.

Use of peptides to determine secondary structure of membrane proteins is becoming widely accepted. Recent studies on transmembrane proteins, including bacteriorhodopsin, rhodopsin, tachykinin receptor, PTH receptor, angiotensin II receptor, α-factor receptor, *β*-adrenergic receptor, band 3, and glycophorin, show that peptides from transmembrane helices form α-helices independently from the rest of the protein (*7*−*18*) and peptides from turns show turns independently of the remainder of the protein (*19*−*25*).

In the approach to membrane protein structure used in this work, all the secondary structure is determined from solution structures of a set of overlapping peptides spanning the sequence of the protein (*20*, *26*). It was hypothesized that with long-range distance constraints from the intact protein, the structures of the peptides could be assembled into a structure of the whole. Superimposing helical structures in the overlapping regions of the peptide structures linked them into a construct corresponding to the whole molecule. Using experimental long-range distance constraints, measured on the intact protein by other methods, to organize the bundle of transmembrane helices, a three-dimensional structure of the membrane protein can be determined. As a verification of this approach, the three-dimensional structure of bacteriorhodopsin was determined. The intrinsic secondary structures of the designed peptides from bacteriorhodopsin agreed well with the X-ray crystal structures. The three-dimensional structure obtained from this technique agreed with previously reported crystal structures of bacteriorhodopsin (*26*). These results open an alternative approach to membrane protein structure, useful in the absence of, or to complement, X-ray crystallography.

We used this approach to address the unanswered structural questions about the cytoplasmic face of rhodopsin in the unactivated and light-activated states. Here we find that the structure of rhodopsin, including the cytoplasmic face, can be determined using solution structures of peptide fragments to define secondary structure and long-range experimental distance constraints from the intact protein to pack the secondary structures into a full tertiary structure. From this work, the structure of the cytoplasmic face of this G-protein receptor is revealed for the first time. In addition the structure of the cytoplasmic face in the activated form of the receptor is also determined. These results reveal some of the conformational changes occurring upon activation of rhodopsin.

† This work was supported by National Institutes of Health Grant EY03328 and NATO.

* To whom correspondence should be addressed. Phone: (860) 486-4363. Fax: (860) 486-4331. E-mail: yeagle@uconnvm.uconn.edu.

[1] Abbreviations: meta II, metarhodopsin II; NMR, nuclear magnetic resonance; PTH, parathyroid hormone.

10.1021/bi015543f CCC: $20.00
Published on Web 09/05/2001

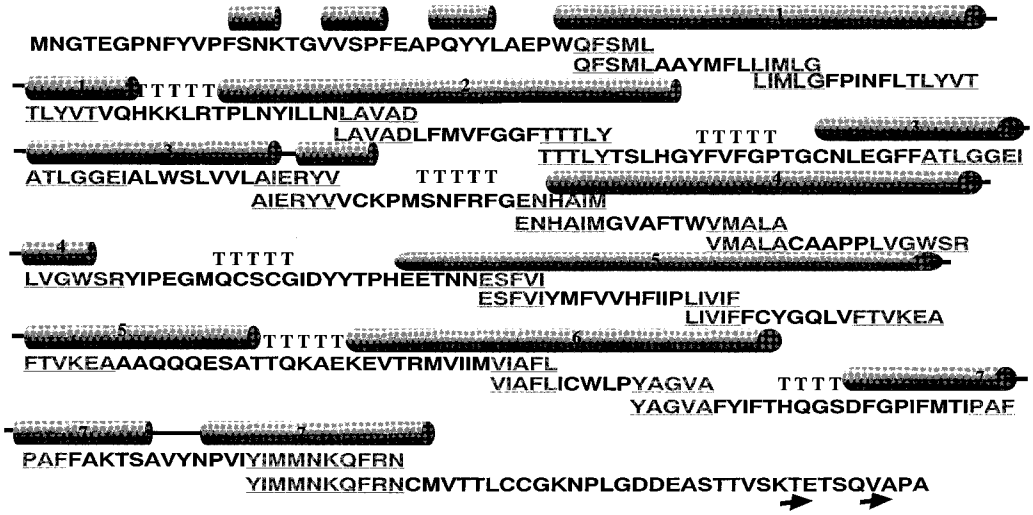

FIGURE 1: Series of overlapping peptides spanning the sequence of rhodopsin. These peptides were designed to contain within each sequence either a turn connecting two helices or a substantial portion of a transmembrane helix. The tubes represent helical regions [numbered in accord with the seven transmembrane segments of rhodopsin (*49*)] and T represents a turn. The arrows indicate short β-strands in the carboxyl terminus.

EXPERIMENTAL METHODS

A series of overlapping peptides spanning the rhodopsin sequence were synthesized (Figure 1). Some peptides were synthesized through solid-phase synthesis in the Biotechnology Center of the University of Connecticut. Synthesis was performed on an Applied Biosystems 433A peptide synthesizer, using fastMoc chemistry on HMP resin at room temperature. HBTU was used for activation and the column was washed with NMP. Some of the peptides were synthesized by Genemed. Mass spectral analysis confirmed the presence of the expected molecular ion. These peptides were purified on HPLC and were greater than 90% pure. The N- and C-termini were not capped. Each peptide was designed to contain either a transmembrane helix or a turn. Each peptide sequence overlapped each of its neighbors. Peptides from the cytoplasmic loops and the carboxyl terminus were soluble in aqueous buffers as reported previously (*22*, *27*). All other peptides were insoluble in water. Some, such as the seventh transmembrane helix, were insoluble in detergent micelles. For these latter peptides, solution structures were determined in DMSO. Previous work had demonstrated that peptides from bacteriorhodopsin in solution in DMSO retained the secondary structure of the native protein (*20*, *26*).

Solution structures of the peptides were determined by two-dimensional homonuclear ^{1}H NMR as described in detail previously. All NMR spectra were recorded on a Bruker AMX-600 spectrometer at 30 °C in DMSO or at 10 °C in water. Standard pulse sequences and phase cycling were employed to record: double quantum filtered (DQF) COSY, and NOESY (data were collected with 400 ms mixing times (*28*). Previous work with other similar-sized peptides at mixing times of 150, 250, and 400 ms showed no evidence of spin diffusion and 400 ms showed the most useful interactions in the NOESY. All spectra were accumulated in a phase sensitive manner using time-proportional phase incrementation for quadrature detection in F1. Chemical shifts were referenced to the residual protons in the d_6-DMSO. Sequence-specific assignments were obtained using standard approaches (*29*). Peptides from turns formed turns in solution (*22*, *27*, *30*) and peptides from helices showed helices that superimposed on the rhodopsin crystal structure (*14*, *15*, *31*).

A construct for the whole protein can be assembled from the pieces whose individual structures are determined as described above. Because of the design of the set of peptides (each peptide overlapped the sequences of its neighbors), the structures in the overlaps of the sequences of these peptides can be superimposed. The superposition was done with recognition of the disordering that is typically observed at the ends of the peptide. The most disordered residues were not used in the superposition algorithm. The unused residues were discarded from the resulting file. The construct then consists of a continuous polypeptide containing the structures of all the peptides with the overlapping sequences. Redundant sequences are then removed from the pdb file.

To K296 11-*cis* retinal was added. Docking of this chromophore was performed after the apoprotein construct was built. The retinal orientation used in our construct is based on solid-state NMR studies (*32*).

On the construct, all the distance range constraints and dihedral angle constraints obtained from the solution structures of each of the peptides were written in a mol2 file with SYBYL (Tripos, St. Louis). Long-range constraints from the intact protein listed in Table 1 were also written on the construct. About half of the distances in the table are determined from dipolar interactions between two spin labels that are covalently attached to the protein at specific sites (engineered cysteine residues). The uncertainty in that measurement for our purpose is the precise location of the unpaired electron that is on the spin label attached to the cysteine. We use as points of origin for the particular distance the most distal hydrogens on the native residues at each of the two positions. This employs an approximation that the spin-labeled residue and the nonlabeled native residue point in a similar direction from the protein backbone. Since these cysteine substitutions have little or no effect on protein function according to the published work (see references in Table 1), the assumption just described seems reasonable. However, because of this approximation and possible dif-

Table 1: Experimental Long-Range Constraints for Rhodopsin[a]

	*R** (Å)	R (Å)
V139C−K248C	23−25	12−14
V139C−E249C	15−20	15−20
V139C−V250C	12−14	15−20
V139C−T251C	23−25	12−14
V139C−R252C	23−25	15−20
H65C−C31 (*50*−*52*)	12−15	7−10
C140−S338 (*53*)	15−21	
V204C−F276C (*54*)	2−5	2−5
I251−V138 (*55*)	<13	
C140−C222 (*56*)	>7	2−5
C140−Q225C	2−5	2−5
K245C−Q312C	>7	2−5
R135C−V250C	>7	2−5
K245C−S338C (*57*)	2−5	2−5
S338C−T242C (*43*)	>7	2−5
Y136C−C222	>7	2−5
Y136C−Q225C	2−5	2−5
interhelical distances (*58*)	X	
helix assignment of Baldwin (*49*)		

[a] Where R* is meta II, and R is rhodopsin (not activated).

Table 2: Interhelical Distance Constraints Used in Simulated Annealing for Rhodopsin (not activated) between the Top, or Middle, or Bottom, of a Pair of Helices, as Described in the Text

amino acids	distance (Å)
Glu 134−Pro 71	9−13
Phe 116−Gly 90	5−10
Ala 153−Pro 71	5−10
Leu 172−Met 86	15−20
Leu 145−Thr 94	18−22
Leu 226−Tyr 136	6−9
Pro 215−Leu 125	6−9
Gln 225−His 152	18−22
Leu 216−Leu 258	9−13
Met 305−Met 253	6−8
Ser 298−Cys 264	6−8
Phe 283−Ile 275	10−11
Ile 286−Met 39	10−13
Gly 114−Tyr 268	14−18
Tyr 268−Pro 171	17−20
Asn 73−Val 250	10−15
Thr 62−Val 250	16−20
Leu 47−Cys 264	16−19

ferences in the length of the normal and modified residues, the distances are converted to range constraints (rather than a specific distance) for use in this structure determination. In the case of disulfides (much of the rest of the list), the distance is defined by the chemistry of the disulfide bond. However, we again convert this distance to a range constraint, because the ability to form a disulfide can bridge a wider interresidue gap (than the final chemistry would indicate) through thermal motion of the protein.

To this were added interhelical distance constraints derived from low-resolution electron diffraction studies (*33*), to define the packing of the helical bundle (center-of-helix to center-of-helix). These constraints consist of distances (as range constraints) between the tops of pairs of helices in the transmembrane bundle, and between the middle and the bottom of pairs of helices of the bundle as well (see Table 2). These distances are then assigned to particular α-carbons on the backbone at the top, middle, or bottom of the transmembrane helices. Using range constraints allows for the possible uncertainty in this assignment of an interhelical distance to distances between specific residues in the helices. Hydrogen bond constraints were added where hydrogen bonds were observed in the original solution structures of the peptides. A simulated annealing protocol was used to fold a structure that was consistent with the available experimental distance constraints. The construct for rhodopsin was heated to 800 °C for 1000 fs and then cooled for 1500 fs to 200 °C. The Kollman All Atom force field and Kollman charges were used within Sybyl. These calculations were performed on a Silicon Graphics R10000 computer.

RESULTS

Structures of the individual peptides from Figure 1 were superimposed to link them together. Usually the overlapping sequences of adjacent peptides showed the same helical structure. Superposition of those helical overlaps (*15*) linked the segments into a construct corresponding to the entire sequence of rhodopsin.

Experimental distance constraints, including 3030 short-range NOE-derived distance constraints from the NMR structure determinations, were written into the mol2 file for this construct. Hydrogen bonds from the peptide structures were added to the construct. Residues 124−131 of helix three and 249−261 of helix six did not show stable intrinsic structures, but were assigned as helical in this construct (*3*, *4*) and are helical in the X-ray crystal structure (*5*). Long-range constraints (Table 1) from independent experiments on intact rhodopsin (unactivated) were written on the construct. Interhelical distances were obtained from the low-resolution electron diffraction studies on two-dimensional crystals of rhodopsin (*3*, *4*). We determined interhelical distances between pairs of helices at the top, middle, and bottom and assigned "top", for example, to a residue near the top of the helix in our construct. These interhelical distances had to be converted to distances between specific α-carbons of specific residues to be included in the constraint list for simulated annealing. This conversion was performed by taking into account the differences between a center-to-center distance for two helices and the distances between atoms on the two helices that are not at the helical center. The distances are range constraints to account for the uncertainties in this procedure (see Table 2). 11-*cis* retinal was constrained by solid-state NMR data (*32*). The construct with the distance constraints was subjected to simulated annealing as described in Experimental Methods. For refinement, additional hydrogen bonds were added when simulated annealing distorted helices from the original peptide structures, and additional cycles of simulated annealing were subsequently performed.

The result, strictly from experimental data, is a compact structure showing a bundle of seven helices connected by six turns (Figure 2A). The transmembrane region of this structure superimposed on the crystal structure with good agreement (rmsd = 1.85, calculated in SYBYL). The environment of the 11-*cis* retinal chromophore in this construct compares favorably with the X-ray crystal structure (*5*) and photocalorimetric studies (*34*). For instance, the *β*-ionone ring is surrounded by aromatic residues (F212, F261, Y268, and W265) from helix V and VI, coinciding with the X-ray structure. The first three of those aromatic residues are believed to be involved in the fine-tuning of chromophore absorption (*34*) and W265 is believed to have

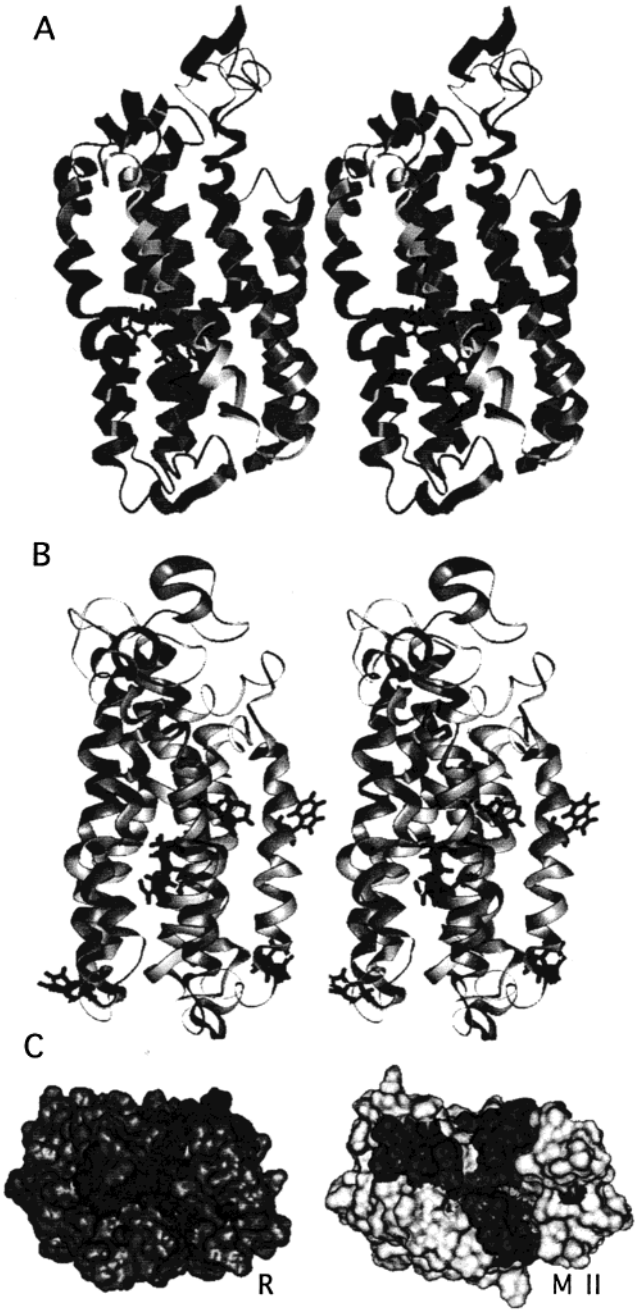

FIGURE 2: Three-dimensional structure of bovine rhodopsin determined as described in the text (PDB ID 1JFP). (A) Ribbon view from the side of the rhodopsin (not activated) structure with the cytoplasmic face up and with each helix colored (helix 1 is red, 2 is brown, 3 is yellow, 4 is green, 5 is light blue, 6 is dark blue, and 7 is purple). The amino terminus is not shown because no experimental long-range distance constraints were available to position the amino terminus in this structure determination. (B) Ribbon diagram viewed from another side, with residues marked as discussed in the text: charged residues in red, and tryptophans with their side chains in dark blue and C322 and C323 with side chains in cyan in upper right of structure. The most likely position of the hydrophobic interior of the lipid bilayer is between these tryptophans. The retinal is in maroon. (C) CPK representation with the structure rotated 90° forward so the cytoplasmic face is observed. The minimal sequences of peptides that inhibit G-protein activation by the receptor, as described in the text, are mapped in red. Major phosphorylation sites (S338 and S343) are colored blue. One phosphorylation site is seen in this view.

steric interaction with the β-ionone ring (*5*). The charged counterion, E113 is within close range of the Schiff base K298. From the β-ionone ring to C_{11}, the retinylidene group runs almost parallel to helix III, in agreement with the X-ray structure. In addition, A117 on helix III is found to be adjacent to the C_9 methyl group of retinal chromophore.

Because the retinal conformation was based on NMR data, this structure inherited the 6-s-trans β-ionone ring orientation instead of the 6-s-cis version shown in X-ray crystallography. Calculations in a recent study (*34*) favored the 6-cis−trans version over the 6-s-cis. Our structure determination cannot distinguish between these possibilities.

Importantly, the cytoplasmic face of rhodopsin is defined, and thus, this new structure of bovine rhodopsin complements the crystallography in which the cytoplasmic face is not observed. The second and third cytoplasmic loops and carboxyl terminus, either not visible or with high *B*-factors in the crystal structure, can be seen in Figure 2A. The structures of the individual components (three loops and the C-terminus) were experimentally defined under conditions where they were biologically active (*22*, *30*). These same components activate transducin separate from the remainder of rhodopsin (*25*). Thus, the intrinsic structures of the cytoplasmic loops and C-terminus are consistent with the native protein.

All helices extend into the cytoplasmic face. The extent of the helices in the third intracellular loop, helix 5 and helix 6, confirm within one residue the model for those helices proposed previously on the basis of atomic force microscopy (*35*). Helix 5 bends over toward helix 6 as it enters the third cytoplasmic loop. The first and second cytoplasmic loops are relatively tight, showing a helix-turn-helix motif in each case. The carboxyl terminal contains two short antiparallel β-strands (residues 335−337, 345−347). This structure is small enough to be captured in the structures determined for the carboxyl terminus [it can be seen in a 19mer (*36*), a 25mer, a 33mer (*30*), and a 43mer (*27*), counting from the true C terminus] even though normally one would not expect β-structures to be seen in the techniques used in this approach to structure determination. The carboxyl terminal shows a fourth cytoplasmic loop with the acylation sites, C322 and C323, at the bottom of that loop. Major phosphorylation sites, S338 and S343, are exposed on the carboxyl terminus. The carboxyl terminus forms the part of the structure most distant from the putative bilayer surface.

The structure suggests the location of rhodopsin in the membrane lipid bilayer. Tryptophans are clustered in the interface between the hydrophobic and hydrophilic regions of membrane proteins (*37*−*39*). Tryptophans (Figure 2B) define a 24−26 Å wide hydrophobic band around the protein. Within this band, only four charged residues are found: one, K296, forms the Schiff base with retinal; second, E113, is the counterion to that Schiff base and located close to it; and third is E122. The hydrophobic band is likely buried in the lipid bilayer. C322 and C323 lie near the inferred membrane surface, consistent with facile acylation of rhodopsin. The receptor mass is likely displaced asymmetrically exposing the cytoplasmic face of the receptor more than the intradiskal face, consistent with the larger number of charged residues in the cytoplasmic face.

The fidelity of this structure is supported by experimental data not used in the structure determination. Protein labeling predicted termination of helix 5 (*40*) and helix 7 (*41*) in agreement with this structure. This labeling also predicted

that residues 227 and 252 point out and residue 250 points in to the helical bundle, as seen in this structure. The short antiparallel β-strands in the carboxyl terminus agree with FTIR data on the intact protein (*42*). Specific interactions between residues 338 and 242 indicate defined structure in the carboxyl terminus (*43*). The third cytoplasmic loop projects toward the carboxyl terminus in agreement with atomic force microscopy data (*35*). The bilayer hydrocarbon thickness inferred from this structure agrees with the width of 20 Å determined from X-ray diffraction (*44*, *45*).

These techniques were next applied to meta II, the transient, light-activated form of this receptor. Table 1 contains a set of experimental distance constraints for meta II. Constraints specifically corresponding to rhodopsin (unactivated) were removed from the construct and constraints for meta II were added. All-trans retinal replaced 11-*cis* retinal. Helices 6, 3, and 4 were allowed to move (by removing interhelical distance constraints), the latter helical movement consistent with a meta II long-range distance constraint between retinal and A169 (*46*). These constraints were written on the structure for rhodopsin (not activated) as the starting point. This construct was subjected to simulated annealing as described in Experimental Methods.

Fewer of the long-range distance constraints from the intact protein were available for the meta II state. Since most of the meta II experimental distance constraints are in the cytoplasmic face, that face is the best-defined part of this preliminary structure. A picture of that face is shown in Figure 2C. By mapping the sequences of peptides from rhodopsin that inhibit receptor−transducin interaction (*47*, *48*) onto the two structures, a putative binding site for transducin on the receptor is identified (Figure 2C). That binding site changes upon activation to meta II. In rhodopsin (not activated), the site is partly occluded and invaginated. More of the putative binding surface is exposed and evaginated in meta II, likely enhancing binding of transducin.

In summary, an experimental three-dimensional structure of rhodopsin (not activated) has been determined and the cytoplasmic face is defined for the first time. At least part of the transducin binding site on rhodopsin is mapped. Conformational changes that occur in the cytoplasmic face upon activation to meta II suggest that the transducin binding site is more exposed in the activated form of the receptor than in rhodopsin (not activated).

REFERENCES

1. Albert, A. D., and Litman, B. J. (1978) *Biochemistry 17*, 3893−3900.
2. Hargrave, P. A., McDowell, J. H., Curtis, D. R., Wang, J. K., Juszczak, E., Fong, S. L., Rao, J. K. M., and Argos, P. (1983) *Biophys. Struct. Mech. 9*, 235−244.
3. Schertler, G. R. X., Villa, C., and Henderson, R. (1993) *Nature 362*, 770−772.
4. Unger, V. M., Hargrave, P. A., Baldwin, J. M., and Schertler, G. F. X. (1997) *Nature 389*, 203−206.
5. Palczewski, K., Kumasaka, T., Hori, T., Behnke, C. A., Motoshima, H., Fox, B. A., Le Trong, I., Teller, D. C., Okada, T., Stenkamp, R. E., Yamamoto, M., and Miyano, M. (2000) *Science 289*, 739−45.
6. Okada, T., Trong, I. L., Fox, G. A., Behnke, C. A., Stenkamp, R. E., and Palczewski, K. (2000) *J. Struct. Biol. 130*, 73−80.
7. Popot, J.-L., and Engelman, D. M. (2000) *Annu. Rev. Biochem. 69*, 881−922.
8. Lemmon, M. A., Flanagan, J. M., Hunt, J. F., Adair, B. D., Bormann, B.-J., Dempsey, C. E., and Engelman, D. M. (1992) *J. Biol. Chem. 267*, 7693−7689.
9. Hunt, J. F., Earnest, T. N., Bousche, O., Kalghatgi, K., Reilly, K., Horvath, C., Rothschild, K. J., and Engelman, D. M. (1997) *Biochemistry 36*, 15156−15176.
10. Pervushin, K. V., Orekhov, V. Y., Popov, A. I., Musina, L. Y., and Arseniev, A. S. (1994) *Eur. J. Biochem. 219*, 571−583.
11. Berlose, J., Convert, O., Brunissen, A., Chassaing, G., and Lavielle, S. (1994) *FEBS Lett. 225*, 827−843.
12. Lomize, A. L., Pervushin, K. V., and Arseniev, A. S. (1992) *Journal of Biomol. NMR 2*, 361−372.
13. Barsukov, I. L., Nolde, D. E., Lomize, A. L., and Arseniev, A. S. (1992) *Eur. J. Biochem. 206*, 665−672.
14. Chopra, A., Yeagle, P. L., Alderfer, J. A., and Albert, A. (2000) *Biochim. Biophys. Acta 1463*, 1−5.
15. Yeagle, P. L., Danis, C., Choi, G., Alderfer, J. L., and Albert, A. D. (2000) *Molecular Vision*, www.molvis.org/molvis/v6/a17/.
16. Arshava, B., Liu, S. F., Jiang, H., Breslav, M., Becker, J. M., and Naider, F. (1998) *Biopolymers 46*, 343−357.
17. Gargaro, A. R., Bloomberg, G. B., Dempsey, C. E., Murray, M., and Tanner, M. J. (1994) *Eur. J. Biochem. 221*, 445−454.
18. Piserchio, A., Bisello, A., Rosenblatt, M., Chorev, M., and Mierke, D. F. (2000) *Biochemistry 39*, 8153−8160.
19. Franzoni, L., Nicastro, G., Pertinhez, T. A., Oliveira, E., Nakaie, C. R., Paiva, A. C., Schreier, S., and Spisni, A. (1999) *J. Biol. Chem. 274*, 227−235.
20. Katragadda, M., Alderfer, J. L., and Yeagle, P. L. (2000) *Biochim. Biophys. Acta 1466*, 1−6.
21. Mierke, D. F., Royo, M., Pelligrini, M., Sun, H., and Chorev, M. (1996) *J. Am. Chem. Soc. 118*, 8998−9004.
22. Yeagle, P. L., Alderfer, J. L., and Albert, A. D. (1997) *Biochemistry 36*, 3864−3869.
23. Yeagle, P. L., Salloum, A., Chopra, A., Bhawsar, N., Ali, L., Kuzmanovski, G., Alderfer, J. L., and A. D. Albert. (2000) *J. Pept. Res. 55*, 455−465.
24. Jung, H., Windhaber, R., Palm, D., and Schnackerz, K. D. (1995) *Febs Lett. 358*, 133−136.
25. Abdulaev, N. G., Ngo, T., Chen, R., Lu, Z., and Ridge, K. D. (2000) *J. Biol. Chem. 275*, 39354−39363.
26. Katragadda, M., Alderfer, J. L., and Yeagle, P. L. (2001) *Biophys. J. 81*, 1029−1036.
27. Yeagle, P. L., Alderfer, J. L., and Albert, A. D. (1996) *Molecular Vision 2*, http://www.molvis.org/molvis/v2/p12/.
28. Kumar, A., Ernst, R. R., and Wuthrich, K. (1980) *Biochem. Biophys. Res. Commun. 95*, 1−6.
29. Evans, J. N. S. (1995) *Biomolecular NMR Spectroscopy*, Oxford University Press, Oxford.
30. Yeagle, P. L., Alderfer, J. L., and Albert, A. D. (1995) *Nat. Struct. Biol. 2*, 832−834.
31. Katragadda, M., Chopra, A., Bennett, M., Alderfer, J. L., Yeagle, P. L., and Albert, A. D. (2001) *J. Pept. Res. 58*, 79−89.
32. Grobner, G., Burnett, I. J., Glaubitz, C., Choi, G., Mason, A. J., and Watts, A. (2000) *Nature 405*, 810−813.
33. Unger, V. M., and Schertler, G. F. X. (1995) *Biophys. J. 68*, 1776−1786.
34. Singh, D., Hudson, B. S., Middleton, C., and Birge, R. R. (2001) *Biochemistry 40*, 4201−4204.
35. Heymann, J. B., Pfeiffer, M., Hildebrandt, V., Kaback, H. R., Fotiadis, D., Groot, B. d., Engel, A., Oestserhelt, D., and Miller, D. J. (2000) *Structure 8*, 643−653.
36. Albert, A. D., Yeagle, P. L., Alderfer, J. L., Dorey, M., Vogt, T., Bhawasar, N., Hargrave, P. A., McDowell, J. H., and Arendt, A. (1997) *Pept.: Chem., Struct. Biol.* (in press).
37. Doyle, D. A., Cabral, J. M., Pfuetzner, R. A., Kuo, A., Gulbis, J. M., Cohen, S. L., Chait, B. T., and MacKinnon, R. (1998) *Science 280*, 69−77.
38. Wallace, B. A., and Janes, R. W. (1999) *Adv. Exp. Med. Biology 467*, 789−799.

39. Yau, W. M., Wimley, W. C., Gawrisch, K., and White, S. H. (1998) *Biochemistry 37*, 14713−14718.
40. Altenbach, C., Yang, K., Farrens, D. L., Farahbakhsh, Z. T., Khorana, H. G., and Hubbell, W. L. (1996) *Biochemistry 35*, 12470−12478.
41. Altenbach, C., Cai, K., Khorana, H. G., and Hubbell, W. L. (1999) *Biochemistry 38*, 7931−7937.
42. Pistorius, A. M., and deGrip, W. J. (1994) *Biochem. Biophys. Res. Commun. 198*, 1040−1045.
43. Cai, K., Langen, R., Hubbell, W. L., and Khorana, H. G. (1997) *Proc. Natl. Acad. Sci. U.S.A. 94*, 14267−14272.
44. Blaurock, A. E., and Wilkins, M. H. (1969) *Nature 223*, 906−909.
45. Gras, W. J., and Worthington, C. R. (1969) *Proc. Natl. Acad. Sci. U.S.A. 63*, 233−238.
46. Borhan, B., Souto, M. L., Imai, H., Shichida, Y., and Nakanishi, K. (2000) *Science 288*, 2209−2212.
47. Konig, B., Arendt, A., McDowell, J. H., Kahlert, M., Hargrave, P. A., and Hofmann, K. P. (1989) *Proc. Natl. Acad. Sci U.S.A. 86*, 6878−6882.
48. Marin, E. P., Krishna, A. G., Zvyaga, T. A., Isele, J., Siebert, F., and Sakmar, T. P. (2000) *J. Biol. Chem. 275*, 1930−1936.
49. Baldwin, J. M. (1993) *EMBO J. 12*, 1693−1703.
50. Yang, K., Farrens, D. L., Altenbach, C., Farahbakhsh, Z. T., Hubbell, W. L., and Khorana, H. G. (1996) *Biochemistry 35*, 14040−14046.
51. Farrens, D. L., Altenbach, C., Yang, K., Hubbell, W. L., and Khorana, H. G. (1996) *Science 274*, 768−770.
52. Gelasco, A., Crouch, R. K., and Knapp, D. R. (2000) *Biochemistry 39*, 4907−4914.
53. Albert, A. D., Watts, A., Spooner, P., Groebner, G., Young, J., and Yeagle, P. L. (1997) *Biochim. Biophys. Acta 1328*, 74−82.
54. Yu, H., Kono, M., McKee, T. D., and Oprian, D. D. (1995) *Biochemistry 34*, 14963−14969.
55. Sheikh, S. P., Zvyaga, T. A., Lichtarge, O., Sakmar, T. P., and Bourne, H. R. (1996) *Nature 383*, 347−350.
56. Yu, H., Kono, M., and Oprian, D. D. (1999) *Biochemistry 38*, 12028−12032.
57. Cai, K., Klein-Seetharaman, J., Hwa, J., Hubbell, W. L., and Khorana, H. G. (1999) *Biochemistry 38*, 12893−12898.
58. Baldwin, J. M., Schertler, G. F. X., and Unger, V. M. (1997) *J. Mol. Biol. 272*, 144−164.

BI015543F